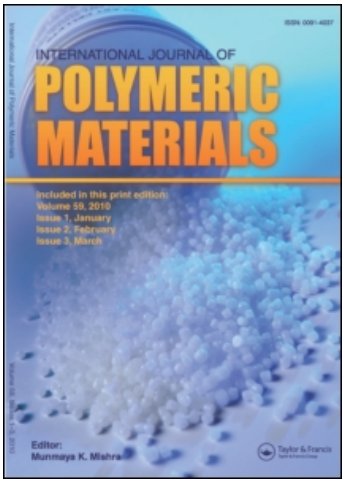

International Journal of Polymeric Materials
Publication details, including instructions for authors and subscription information:
http://www.informaworld.com/smpp/title~content=t713647664

Effect of Molecular Weight on the Strength of Nylon 6 and PET Fibers

D. C. Prevorsek[a]; R. H. Butler[a]
[a] Allied Chemical Corporation, Morristown, N.J.

To cite this Article Prevorsek, D. C. and Butler, R. H.(1973) 'Effect of Molecular Weight on the Strength of Nylon 6 and PET Fibers', International Journal of Polymeric Materials, 2: 3, 185 — 203
To link to this Article: DOI: 10.1080/00914037308075309
URL: http://dx.doi.org/10.1080/00914037308075309

Intern. J. Polymeric Mater., 1973, Vol. 2, pp. 185–203

Printed in Great Britain

Effect of Molecular Weight on the Strength of Nylon 6 and PET Fibers

D. C. PREVORSEK and R. H. BUTLER

Allied Chemical Corporation, Morristown, N.J. 07960

(*Received December 15, 1972*)

INTRODUCTION

The mechanical properties of polymers depend on their morphological characteristics. With many systems and especially with semicrystalline polymers, it is possible to achieve significant changes in structure and properties by varying their thermal and stress histories. Considering the broad range of polymer applications it would, therefore, be desirable to have a quantitative understanding of the effects of structure on the properties of polymers in the solid state. The morphology of polymers is, however, often so complex that the interpretation of the mechanical responses must be restricted to qualitative considerations. In particular, the analysis of strength of unoriented semicrystalline polymers is quite complex because of large plastic deformations which usually precede the rupture. However, by orienting the polymers in the form of fibers, it is possible to achieve structures which can be ruptured in tension with minimum plastic deformation. Under these conditions, the analysis of mechanical properties is greatly facilitated for fibers. Nevertheless, we still lack a quantitative understanding of the mechanical responses of polymeric fibers mainly because their structure has not yet been described with a precision allowing rigorous treatments.

Many polymers in fibrous form exhibit the characteristics of two-phase systems. Therefore, their mechanical responses depend on the properties of each phase, morphological characteristics of the two-phase system, and on the structure of the phase boundaries. To date, the morphological studies based on the examination of unstrained samples give a very inconclusive picture regarding the structure of the interphase which affects the mechanical coupling between phases.

Since the properties of the crystalline phase can be estimated from molecular and crystallographic data it should be possible to determine the load transfer characteristics between phases from the analysis of the mechanical responses. Considering that under these conditions a combined mechanical and structural analysis could lead to a better understanding of the structure of the crystal surfaces in fibers, it was decided to examine by this technique a series of Nylon 6 (N6) and Poly(ethylene terephthalate) (PET) fibers. In the course of this work, we arrived at several unexpected findings which prompted additional investigation.

In the calculations concerned with the theoretical strength of a parallel array of polymer molecules we found that with extended molecules the strength increases monotonically with the molecular weight and that the cohesive energy does not effect the maximum theoretical strength. With the folded chains, however, the plot of strength vs. molecular weight reache a maximum at a value of number average molecular weight which equals that of the number average molecular weight between the folds. Since further increases in the molecular weight lead to a reduction in strength, the maximum theoretical strength of systems which include chain folding is affected by the cohesive energy.

Our studies also indicated that the cohesive energy of an oriented polymer could be estimated from the plots of strength as a function of the molecular weight. Since the cohesive energy between the molecules is strongly affected by the intermolecular distance, it was speculated that, in principle, the examination of a series of fibers of various molecular weights could lead to estimates of the density of the load-bearing phase and the degree of chain folding. Realizing that this information cannot be obtained by other methods, it was decided to undertake such a study in spite of difficulties expected in the preparation of an adequate series of fibers of various molecular weights.

In this paper we review the theoretical background and present the results derived from the analysis of the effect of molecular weight on the strength of PET and N6 fibers.

THEORY

Fibers subjected to large longitudinal strains often display microscopically visible "strain bands".[1,2] Although the structure of these bands has not yet been described in detail, there is evidence that the bands involve internal cavities or other structural features of lower density. Since many of the observations concerning strain bands resemble those expected for microcracks, the cavities in the band can be regarded as the precursor of the crack which leads to rupture of the specimen.

In the development of a theory of tensile strength, which assumes that the rupture of fibers is a result of the formation and propagation of a crack across the fiber, it is important to consider the fact that the fiber structure remains stress-sustaining even in the stage where the microcracks are formed. Thus, we must distinguish between the cracks which are stable and require energy for further growth, and those which are unstable and grow spontaneously. The difference between the two phases in the crack growth can be observed on notched fibers ruptured in tension.[3]

In Figure 1 are shown the top and the side views of a Nylon 6 fiber (28 mm diameter) whose rupture in tension was initiated from a circumferential

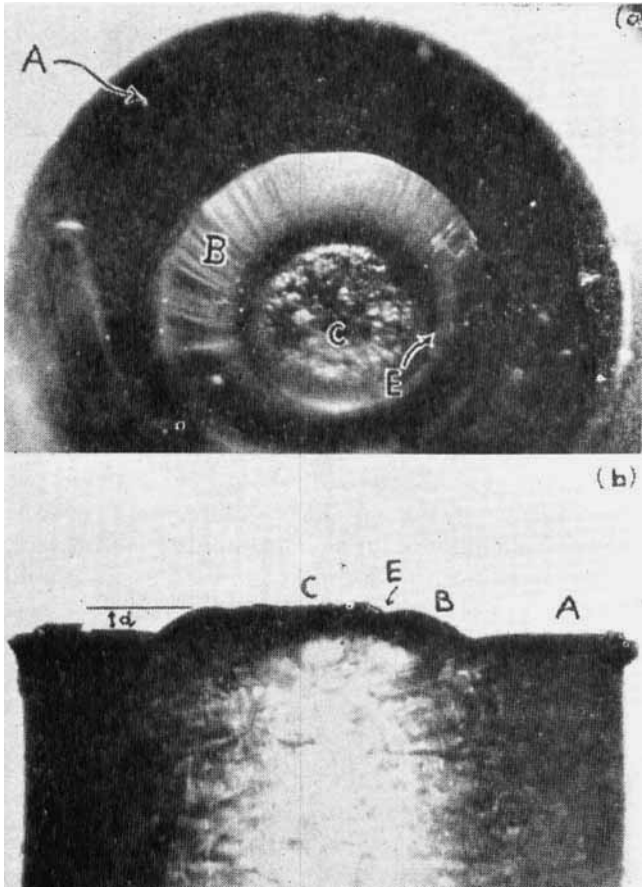

FIGURE 1 Top (a) and side (b) views of a broken Nylon 6 monofil ruptured in a tensile test. Fracture initiated from a circumferential notch.

notch. With regard to appearance, the surface of the broken end can be divided into three areas. The area cut with the blade (A) usually shows some roughness and traces of the knife. The area formed during the slow propagation of the crack (B) is very smooth and rises considerably above the level of the area cut with the knife. The distance "d" indicated in Figure 1(b) reflects the magnitude of the plastic deformation occurring during rupture. The central area (C) formed during the rapid propagation of the notch at the instant of rupture is rough and is separated from area (B) by a narrow valley (E). It is believed that this valley is formed as a result of a sudden release in stress energy when the fiber is ruptured. Thus, the diameter of the valley is probably an indication of the critical depth of the notch, which should be regarded as the analog of the critical size of the crack discussed below.

Although the propagation rates of unstable cracks in fibers have not yet been determined, it is quite certain that these rates are several orders of magnitude higher than those of the growth of the stable cracks. Therefore, the time to form an unstable crack is much larger than the time involved in the propagation of unstable crack across the specimen. Consequently, the expressions of strength or time to break can be derived from the expressions defining the time to form an unstable crack.

The conditions of crack stability and its critical size depends on the material properties and the geometry of crack. Therefore, for a specific case, a rigorous treatment of strength can only be formulated on the basis of a complete description of the geometry of the stable crack. Unfortunately, the examination of the ends of fibers ruptured in tension reveals primarily only the features formed in the process of the spontaneous growth of the crack. Thus, the pertinent information regarding the geometry of the stable crack can only be obtained from fibers strained short of rupture. These studies are, however, quite involved because with many fibers the fracture is initiated from the cracks formed in the interior of the fiber and not from the surface. Thus, it is not surprising that at present we still lack a detailed description of stable cracks for various specific cases.

Considering this lack of information, it is desirable to derive a general model, in which crack geometry is in agreement with the prevailing data is assumed. Following this rationale we presuppose in the developments below that the cracks are circular, flat and perpendicular to the applied stress.

The free energy associated with the formation of such a crack of radius r is given by Sack.[4]

$$\Delta f_r = 2\pi r^2\rho - 8(1 - \mu^2)r^3\sigma^2q^2/3E. \tag{1}$$

In this expression ρ is the surface energy, defined as the work required to form unit area of surface in a brittle material by formation of two planes each half unit in area, σ is the applied tensile stress, q is the stress concentration factor,

E is Young's modulus, and μ is Poisson's ratio. The curve of Δf_r versus r has a maximum for cracks with radius $r^* = \rho E/2(1 - \mu^2)q^2\sigma^2$. As soon as this radius is exceeded, the crack becomes unstable and the specimen fractures catastrophically.

The growth of cracks may be regarded as a process in which polymer chain segments are transferred from the state in which all segments are completely surrounded by like segments (the α state) to the surface of cracks (the β state). If the growth of cracks is regarded as a thermally activated process, then their rate of growth R_r can be written as

$$R_r = \frac{kT}{h}\left[n_r Z_r \exp\left\{\frac{\Delta F_1^*}{kT} + \frac{vq^2\sigma^2}{2EkT}\right\} - n_r' Z_r' \exp\left\{ - \frac{\Delta F_2^*}{kT} - \frac{vq^2\sigma^2}{2EkT}\right\}\right]. \tag{2}$$

In this expression, k and h are the Boltzmann and Planck constants, respectively, T is absolute temperature, E is Young's modulus, r and r' represent the radius of a crack before and after a segment of a polymer chain is transferred from the standard state to the surface of the crack. n_r is the number of α segments in contact with each nucleus of size r, and Z_r is the steady-state concentration of β_r nuclei. $n_r Z_r$ is, therefore, the steady-state concentration of α segments available for reaction. ΔF_1^* is the free energy of activation associated with the separation of two segments of a polymer chain or chains, as the edge of the crack moves between them. n'_r is the number of β segments in contact with the standard state in a nucleus having radius r'. Z_r' is the steady-state concentration of cracks having radius r' and ΔF_2^* is the free energy of activation associated with the elimination of a vacancy between two segments. $q^2\sigma^2/2E$ is the strain–energy density in the vicinity of the crack, (where q is a stress concentration factor and σ is the stress) and v is the effective volume of the vacancy created by the separation of two chain segments. The term $vq^2\sigma^2/2E$, therefore, represents the work done by the applied stress in one step of the crack–propagation process. R_r is in terms of the number of chain segments participating in crack growth throughout unit volume of the specimen, in unit time. The number of α segments n_r in contact with each nucleus at the apex of a crack β_r is not strictly equal to the number $n'_{r'}$ of β segments in contact with the standard state at the apex of a β_r nucleus. However, the difference is expected to be small, so that it can be assumed that $n_r = n'_{r'}$. Since the experiments to which this theory could apply are performed at temperatures at which the mobility of molecules is low, n_r must be of the order of magnitude of the number of polymer chains $2\pi r/l$ in contact with the apex of the circular crack having radius r, where l is the mean distance between polymer chains in direction perpendicualr to the fiber axis. According to a

treatment proposed by Prevorsek and Lyons,[5] the expression (2) can be simplified as follows:

$$R_r = (2kT\pi rZ/hl)\exp\{ - (\Delta f_r/kT) - (\Delta F^*/kT) + (vq^2\sigma^2/2EkT)\} \quad (3)$$

where Δf_r equals free energy associated with the formation of a crack having radius r, and ΔF^* is an intermediate value between ΔF_1^* and ΔF_2^*.

According to Eqs. (1) and (3) the rate of crack growth depends on the radius of the crack and decreases as the crack approaches its critical size. Taking into account that, in a sequence of changes differing considerably in rates, the net rate is that of the slowest step in the sequence, then the rate of formation of cracks having the critical size, i.e. cracks of radius r^*, can be approximated by

$$R_r^* = \frac{2kT\pi r^*Z}{hl}\exp\left\{\frac{1}{kT}\left(- \Delta f_r^* - \Delta F^* + \frac{v\sigma^2q^2}{2E}\right)\right\} \quad (4)$$

with

$$\Delta f_r^* = \pi^3\rho^3E^2/6(1 - \mu^2)^2q^4\sigma^4.$$

Assuming further that the number of polymer chain segments that must be brought to the surface of a crack in the rate-controlling step to produce instability is of the order of magnitude of $2\pi r^*/l$, the rate of initiation of an unstable crack becomes

$$R_c = (l/2\pi r^*)R_r^*. \quad (5)$$

If, as experimental results appear to indicate, the rate of failure (number of failures per unit time) can be regarded essentially as the rate of initiation of an unstable crack, then an expression for the expected lifetime t_b of a specimen under constant stress, can be derived as follows:

$$\begin{aligned} t_b &= 1/R_cV \\ &= 2\pi r^*/lVR_r^* \\ &= (h/kTZV)\exp(1/kT)[\Delta f_r^* + \Delta F^* - (vq^2\sigma^2/2E)] \end{aligned} \quad (6)$$

where V is the volume of the specimen.

In proceeding to an expression for the time to failure in a tensile test, we apply the linear rule of cumulative damage (6) which under conditions of time dependent stress assumes the form

$$\int_0^{t^*} \frac{dt}{t_b[\sigma(t)]} = 1 \quad (7)$$

where t^* is the time to failure. The validity of Eq. (7) has been established both theoretically[7] and experimentally[8] for conditions where $\sigma(t)$ increases monotonically with time.

It follows from Eqs. (4), (5), (6) and (7) that

$$\frac{VZkT}{h}\exp\left(-\frac{\Delta F^*}{kT}\right)\int_0^{t^*}\exp\left\{\frac{1}{kT}\left[\frac{v\sigma^2(t)}{2E}-\frac{\pi^3\rho^3E^2}{6(1-\mu^2)^2\sigma^4(t)q^4}\right]\right\}dt=1. \tag{8}$$

In a tensile test performed at a constant rate of increase of stress,

$$\sigma(t)=\dot{\sigma}t$$

where $\dot{\sigma}$ is the rate of stressing, and

$$\frac{VZkT}{h}\exp\left(-\frac{\Delta F^*}{kT}\right)\int_0^{t^*}\exp\left\{\frac{1}{kT}\left[\frac{v\dot{\sigma}^2t^2}{2E}-\frac{\pi^3\rho^3E^2}{6(1-\mu^2)^2\dot{\sigma}^4t^4q^4}\right]\right\}dt=1. \tag{9}$$

The upper limit of the integrals in Eqs. (7), (8), and (9), t^*, is the time to failure in a tensile test. Breaking stress σ^* can then be calculated from

$$\sigma^*=\sigma t^*. \tag{10}$$

The Eqs. (6) and (9) include the four primary parameters which are affected by the molecular structure of the polymer: modulus, activation energy associated with the processes involved in the crack growth, fracture surface energy and the concentration of the crack nucleation sites.

The modulus of elasticity appearing in the equations of strength can be derived from the modulus of polymer crystals in the principal chain direction.[9-13] For a specified molecular and crystallographic structure this modulus may be calculated from the force constant for bond stretching and valence angle deformation derived from vibration frequencies of molecules. Direction cosines, bond angles and the effective cross-sectional areas of the polymer chains are derived from the x-ray measurements. The moduli of crystallites in fibers have also been determined experimentally by measuring the crystal lattice strains in samples under load.[14,15]

In connection with these studies it must, however, be noted that the determination of crystal moduli from the lattice strain measurements cannot be made without an independent determination of the mechanical coupling between the amorphous and the crystalline phase (series, parallel or a series–parallel combination). This important step has been omitted in all studies of crystalline moduli published to date. Since in the analysis of their experimental data, all authors assumed a series type of coupling between phases, we must regard these results as the lower bound of modulus. It seems, however, that in most cases the error may not be large because the recent studies along these lines indicate that with many fibers the load transfer characteristics between phases approach rather closely to those of a series model.[16]

From mechanical considerations it is expected that straining of an ensemble of parallel molecules should lead primarily to the scission of the weakest bonds in the polymer chain. This hypothesis has been confirmed by Zhurkov[17] in a study in which the activation energies associated with the breakdown of highly oriented polymers were extracted from the data of time to break as function of temperature. The fact that the activation energies determined in mechanical experiments agree well with those associated with processes of thermal degradation indicates that under certain conditions these two processes could be very similar.

In the analysis of the data of strength with regard to the activation energy of the mechanical breakdown it must, however, be remembered that the process of crack growth involves very probably both chain scission and chain slippage. Considering that the relative importance of these two processes should depend on the average chain length and the cohesive energy of the system, it is expected that the activation energies of breakdown are strongly dependent on the temperature and the molecular weight of the polymer.

The choice of a value for the concentration of the nucleation sites can at present be made only by speculation. We believe that the phase boundaries between the crystallites and the "amorphous phase" are the most likely sites for the formation of the microcracks. Consequently we assume that the concentration of nucleation sites is of the order of magnitude of the concentration of crystallites.

The experimental methods to study the fracture surface energy (FSE) are not suitable for the examination of specimens in the form of fibers. Thus, the considerations of this molecular weight dependent parameter must rely at present entirely on the theoretical calculations. A systematic study of FSE as a function of molecular weight, bond and cohesive energies, and degree of chain folding has been carried out recently for ensembles of parallel molecules.[18] In the calculations, it was assumed that: (1) the polymer molecules are linear and oriented parallel to the fiber axis, (2) the arrangement of chain ends and chain folds in the fiber is random, (3) the path of a crack is such that an increment in its size leads to a maximum release in strain energy, and (4) the crack can grow either by chain scission or by chain slippage depending on which is energetically more favorable. Plots of FSE vs. molecular weight led to the following observations which are pertinent for the analysis of the experimental data below.

With fully extended molecules, FSE increases monotonically with the molecular weight and approaches asymptotically its maximum value

$$(\mathrm{FSE})_{\max} = N \times Q_B$$

where N = number of molecules per unit cross-sectional area and Q_B = the energy to break the weakest bond in the polymer chain. The cohesive energy

Q_L while not contributing substantially to strength at high values of the molecular weight affects strongly the minimum molecular weight required for processing and the width of the molecular weight range where strength is molecular weight dependent. FSE of systems containing folds distributed randomly in the volume of the specimen is lower than that calculated for a fully extended chain. Plots of FSE as a function of D_p (degree of polymerization) for various levels of chain folding, expressed as average chain length between the folds, show a maximum at a D_p corresponding approximately to the average length (average D_p) between the folds. Consequently for a given polymer system characterized by a set of values of N, Q_B and Q_L the maximum in FSE is a function of the degree of chain folding. Typical plots of FSE as a function of the degree of polymerization showing the effects of cohesive energy and chain folding are shown in Figure 2.

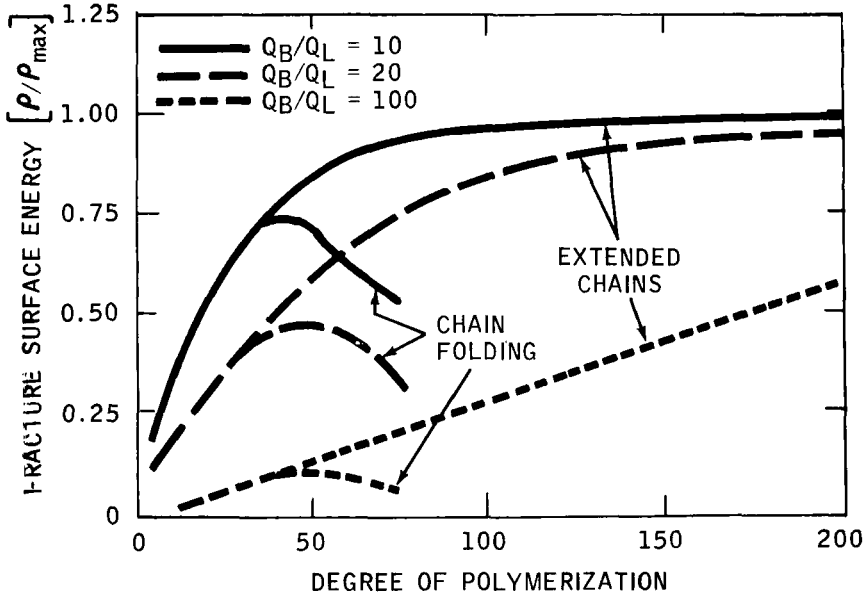

FIGURE 2 Fracture surface energy (FSE) as function of degree of polymerization (D_p); effects of cohesive energy and chain folding (average length between the folds in units of $D_p = 50$).

EXPERIMENTAL

In order to study the effect of molecular weight on the strength of highly-oriented N6 and PET fibers, it was necessary to prepare a series of fibers with nearly equal structural characteristics which differed only in molecular weight.

For this purpose, a series of Nylon 6 and poly(ethylene terephthalate) polymers of different molecular weight were melt-spun and drawn into 12 filament low-denier yarns. The respective ranges in number average molecular weight of the experimental PET and N6 polymers were 8,000–31,000 and 10,000–50,000. Yarns of highest strength were submitted for structural characterization with regard to degree of crystallinity, amorphous, and crystalline orientation. With several fibers we observed a remarkable similarity in structure on the first trial. With those fibers showing structural differences, the required modifications were achieved by small adjustments in the draw ratio. With PET samples having M_n of 8,000 and 9,500 and with N6 samples having M_n of 10,000 and 50,000, we were, however, unable to prepare fibers acceptable for the analysis in spite of considerable effort in the adjustments of processing conditions.

The number average molecular weights of N6 and PET fibers with sufficient structural similarity to be considered in the analysis below are summarized in Table I.

TABLE I

Number average molecular weight of experimental N6 and PET fibers

PET	N6
13,300	18,000
21,000	22,000
26,300	27,000
30,500	

In order to alter the degree of chain folding in these fibers[19] with a minimum effect on the degree of crystallinity and crystalline orientation, we allowed the fibers to contract under tension for 10 and 20 percent. The treatment involved a three-second exposure of yarns to a block heater maintained at 225°C for PET and 170°C for N6 fibers. The fully drawn and contracted PET fibers had a degree of crystallinity (by x-ray) of 56 $\pm$ 1% and a crystalline orientation expressed as the half azimuthal angle of 105 reflection of 11–12°. The N6 fibers, on the other hand, had an x-ray crystallinity of 71 $\pm$ 1% and a crystalline orientation corresponding to 9–10 degrees in half angles of (200) and (202 + 002) reflections. The similarity in structure of the fully drawn fibers is further illustrated in Figures 3 and 4 by the presentation of their respective stress–strain diagrams obtained at −100°C.

RESULTS AND DISCUSSION

The theory discussed above assumes that the effects of plastic deformation are negligible in the fracture process. Consequently, we shall base our analysis

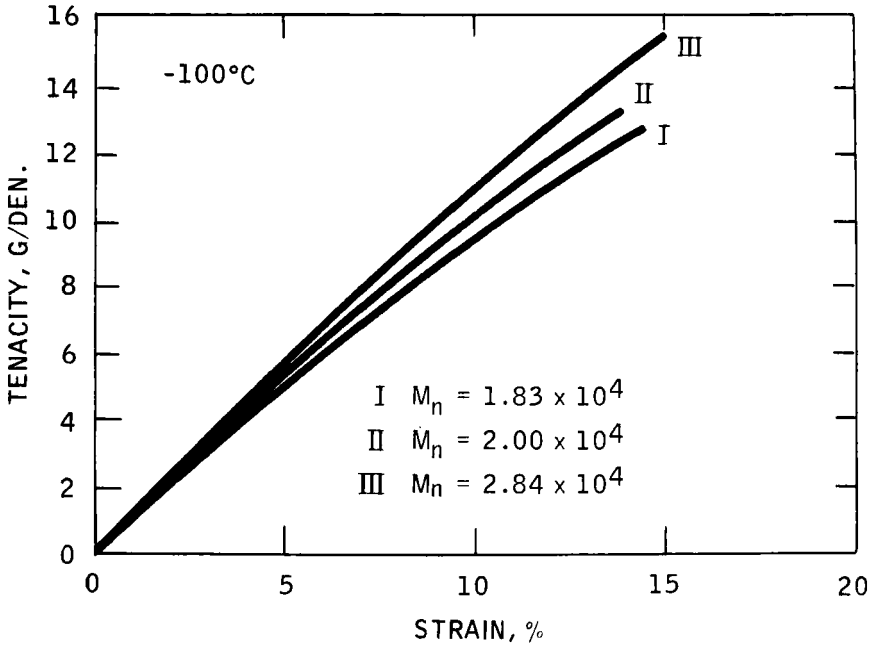

FIGURE 3 Stress–strain diagrams of experimental unrelaxed Nylon 6 fibers.

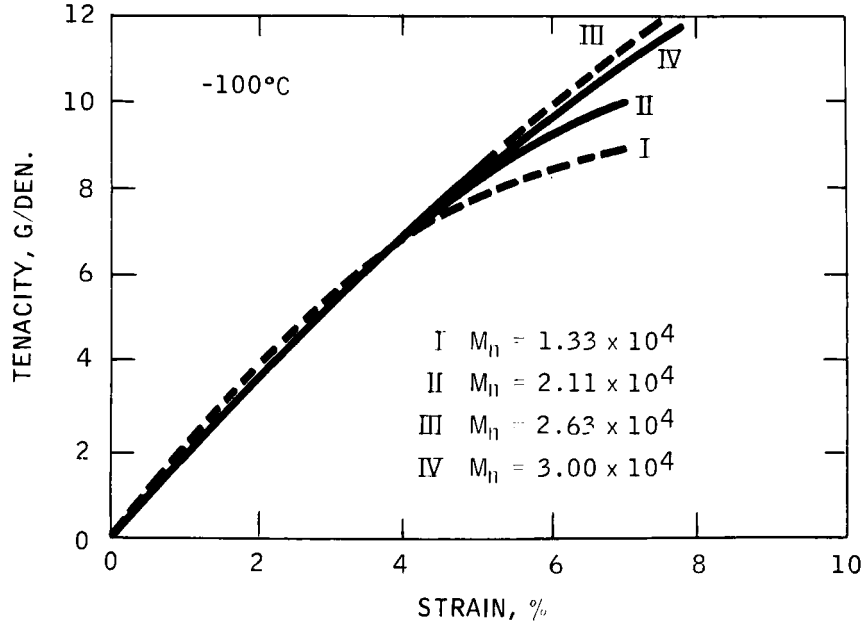

FIGURE 4 Stress–strain diagrams of experimental unrelaxed PET fibers.

primarily on the results from fully drawn samples ruptured at −100°C. The results of contracted samples and data obtained at 23°C are included primarily for a qualitative comparison.

The effects of molecular weight and temperature on fully drawn PET fibers and those contracted for 10% are shown in Figure 5. The strength in this

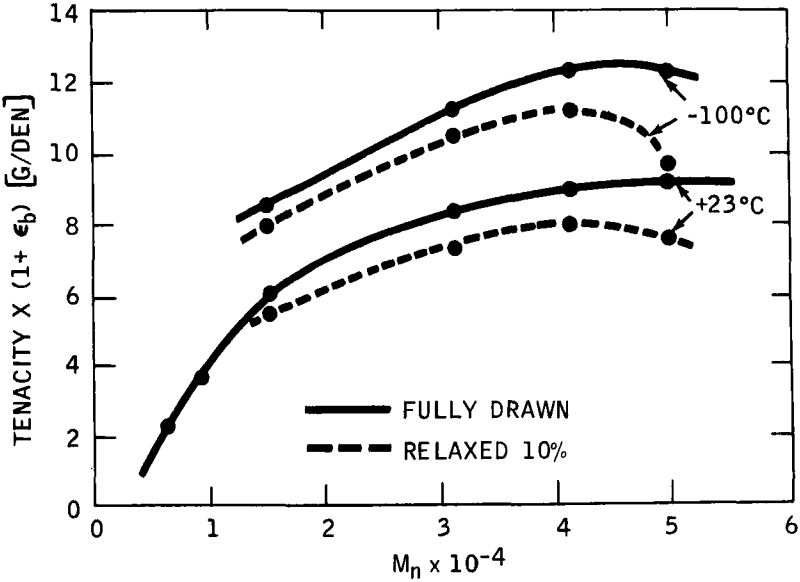

FIGURE 5 Tenacity of PET fibers: effects of molecular weight, temperature, and relaxation.

graph and those that follow is expressed in tenacity corrected for the increase in fiber length before rupture. The strength of these fibers increases monotonically with the molecular weight in the investigated range of M_n. The temperature, while lowering the strength, does not affect this general observation. PET fibers contracted for 10% behave differently. The respective plots of strength vs. M_n indicate a distinct maximum in strength at an M_n of ~26,000 both at 23° and −100°C. Although not shown on the graph, it should be noted that the samples contracted for 20% also show maximum in strength at an M_n ~26,000.

The effects of molecular weight and temperature on strength of fully drawn and thermal contracted N6 fibers are shown in the plots in Figure 6. The strength of fully drawn samples show a broad maximum at an M_n of 30,000. Considering that the fiber having an M_n of 50,000 showed some irregularities on its surface (not noticed with the other fibers of this series) we regard the

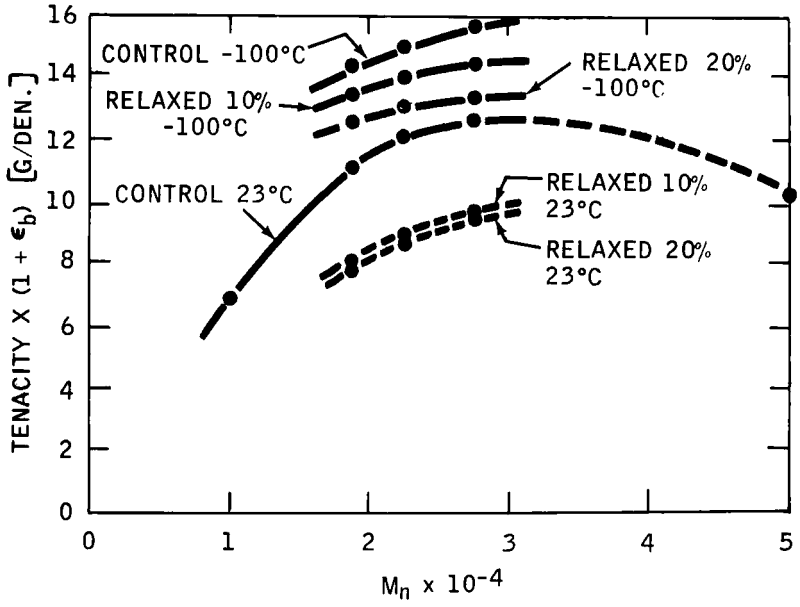

FIGURE 6 Tenacity of N6 fibers: effects of molecular weight, temperature, and relaxation.

data of strength at $M_n = 50{,}000$ as questionable. The examination of the plots in the range of M_n between 18,000 and 30,000 where our results are considered acceptable for analysis, indicates a behavior very similar to that observed with the PET fibers. For example, the data at −100°C indicate that with the fully drawn samples the strength increases in the M_n range between 20,000 and 30,000. With the contracted samples, on the other hand, a levelling of strength is observed already at an M_n of about 20,000.

An interpretation of these data on the basis of the theoretical results discussed above, namely, that the fiber strength is expected to reach its maximum near a value of M_n in strength which equals approximately the M_n between the folds, one arrives at the following conclusions:

1) The behavior of fully drawn N6 and PET fibers resembles that of a structure containing random chain folding with the average distance between the folds exceeding an M_n of 30,000.

2) Thermal contraction increases the degree of random chain folding to a level corresponding to an average distance between the folds of about 20,000 to 25,000.

In the interpretation of data from contracted samples it must be kept in mind that these samples rupture at significantly higher strains than the unshrunk fibers. Thus, these results preclude a quantitative interpretation. It

can, however, be speculated that the straining of folded molecules under tension can only lead to an increase in the average distance between the folds. Thus, we believe that with the contracted samples the degree of chain folding is probably higher than the plots of strength vs. the molecular weight.

In order to proceed with the analysis and to estimate the cohesive energy of the load-bearing phase of the fibers it is necessary to calculate the theoretical strength of an ideal ensemble of N6 and PET molecules as a function of the molecular weight by means of the Eq. (9). The values of parameters used in these calculations are listed in Tables II and III.

TABLE II

Numerical values of parameters used in calculation of theoretical strength of N6 and PET fibers

Temperature T, K	300, 170
Poisson's ratio μ	0.4
Volume of specimen V, cm^3	3×10^{-5}
Concentration of nucleation sites Z, cm^{-3}	10^{19}
Volume of an elementary vacancy v, cm^3	2×10^{-23}
Average distance between polymer chains l, cm	5×10^{-8}
Stress concentration factor q	1
Stress rate $\dot{\sigma}$, dyne/cm^2-sec	1×10^2

In the absence of data regarding the activation energy associated with the mechanical breakdown of PET we assumed that the 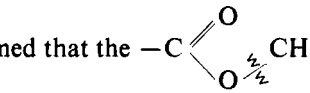 bond is most likely to undergo scission under stress. Under these conditions it is expected that both N6 and PET should have an activation energy of about 3.13×10^{-12} ergs/bond. The moduli of N6 and PET crystals in the direction of the polymer chain were calculated[10,11] and measured experimentally.[14,21] The results of Table III indicate that the calculated values are somewhat higher than those measured experimentally, nevertheless, the agreement is reasonable. In the calculations we used the values determined experimentally.

The fracture surface energy as a function of molecular weight was calculated using a Monte Carlo technique. These calculations require the knowledge of the breaking energies of an isolated polymer chain, number of molecules intersecting a unit area and specific cohesive energy. The values of the breaking energies of N6 and PET molecules have already been discussed. Values of cohesive energies were estimated by means of the additive schemes prepared by Bunn[20] while the number of molecules intersecting a unit area were calculated from the x-ray data.

Plots of fracture surface energy calculated using parameters listed in

TABLE III

Data used in calculations of theoretical fracture surface energy and strength of N6 and PET fibers

		PET	N6
Modulus (dyne/cm²)	X-ray	7.5×10^{11}	2.4×10^{11}
	Calculated	1.2×10^{12}	1.9×10^{12}
	Fiber	2.2×10^{11}	0.8×10^{11}
Weakest bond		—C—O—	—C—N—
Bond energy (ergs/bond)		3.13×10^{-12}	3.13×10^{-12}
Specific cohesive energy (crys/5A)	Crystal	3.5×10^{-13}	3.6×10^{-13}
	Fiber	3.1×10^{-13}	3.5×10^{-13}
Density	Crystal	1.455	1.175
	Fiber	1.34	1.145
Number of molecules per unit area (N/cm²)	Crystal	4.9×10^{14}	5.7×10^{14}
	Fiber	4.5×10^{14}	5.6×10^{14}

Table III are shown in Figure 7. In the calculations it is assumed that average distance between the folds is 1800Å as indicated by our experimental data. It is interesting to note that the fracture surface energy of N6 is considerably higher than that of PET despite the fact in the form of an isolated chain we

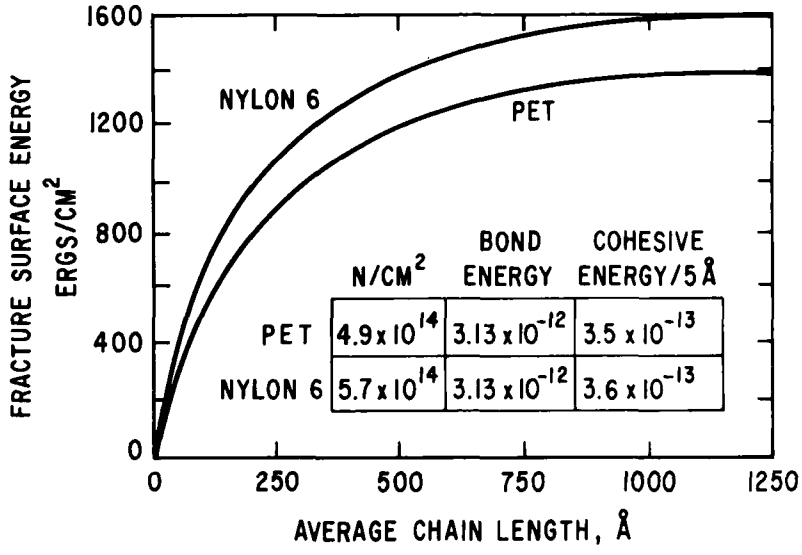

FIGURE 7 Fracture surface energy of uniaxially oriented N6 and PET.

c

assumed that both polymers had equal strength. The difference in the FSE of an ensemble of molecules is due to the fact that N6 has more molecules intersecting the fracture plane than PET.

When values of ρ, E and ΔF discussed above are used in Eq. (9) one obtains the plots of strength vs. molecular weight shown in Figure 8. The theoretical strength of PET is higher than that of N6 because of the higher modulus of PET. In Figure 8 are shown also the data of strength measured with experimental fibers discussed above.

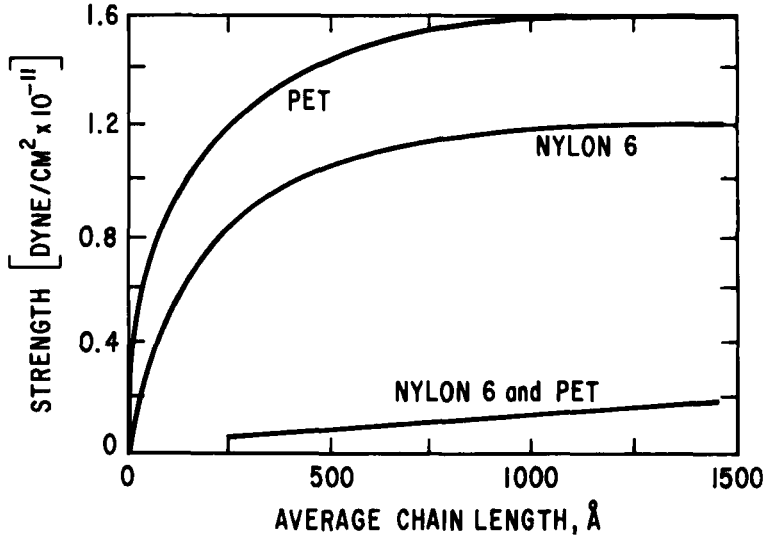

FIGURE 8 Theoretical and observed strength of uniaxially oriented N6 and PET.

The outcome of these calculations, namely, the finding that the theoretical strength of fibers is about an order of magnitude higher than that of the experimental fibers is not surprising. There is ample evidence derived from the morphology studies that these fibers must be regarded as a two-phase system. Arguments in favor of this concept will now be derived from the analysis of data of strength. It was shown that the slope of FSE vs. molecular weight is a function of the cohesive energy of the system. Consequently, the cohesive energy of an oriented polymer can be extracted from the data of strength vs. molecular weight if the data are plotted in terms of the fraction of maximum observed strength. When this method is applied to our experimental data and compared with curves calculated by means of Eq. (10), we obtain the results shown in Figure 9. The fact that the curve calculated using a value of cohesive energy estimated for a one-phase PET system having the density of experimental fibers is much steeper than those representing the experimental

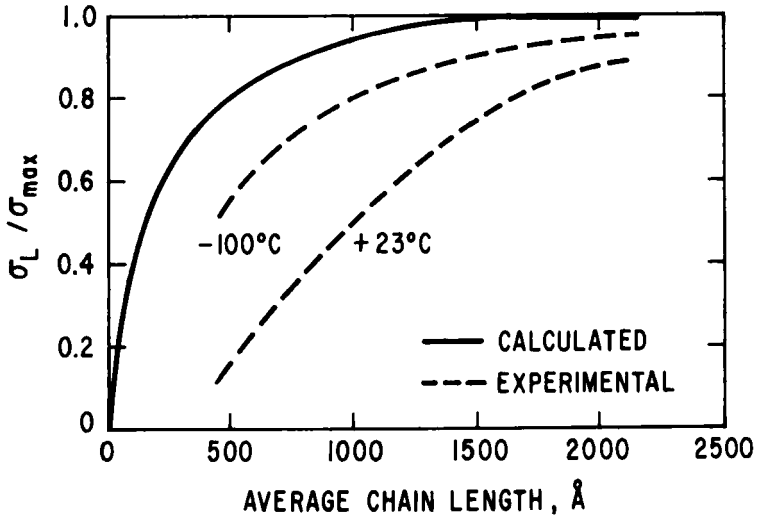

FIGURE 9 Reduced calculated and observed strength σ/σ_{max} of uniaxially oriented N6 and PET.

data obtained at −100°C and +23°C indicate that the fibers behaved as if they had a much lower cohesive energy than the experimental fibers. Considering the strong dependence of cohesive energy on density and the change in the slope resulting from a decrease in temperature, it is reasonable to assume that the observed discrepancy between the calculated and measured data results from the fact that the load-bearing phase in fibers has a lower density than the fibers.

From the considerations of the effects of density on strength, it can further be inferred from these results that the strength determining lower density phase is also the weaker phase of the system. This rather trivial conclusion leads to a series of important implications regarding the fiber structure if this information is interpreted in terms of the mechanical coupling between the phases. By invoking the effects of a series or a parallel coupling between the phases on the properties of the system, it follows that these data strongly indicate a series coupling between the phases, which in turn implies that the weaker phase forms the matrix of the system. Considering further the effects of length to diameter ratio of a stronger dispersed phase on the strength and modulus of the two-phase composite we must conclude that the crystallites in these fibers cannot appear in the form of rods whose length to diameter ratio significantly exceeds two.

The absence of a maximum in strength with fully drawn unrelaxed fibers in the range of the investigated molecular weights and its implications regarding

the degree of chain folding must now be reversed. Since we arrived at the conclusion that these fibers have a two-phase structure with only one phase contributing substantially to strength, the inferences regarding chain folding must not be applied to the system as a whole, but to the phase which has an overriding effect on strength. Thus, we arrive at an important conclusion of this work, namely, that the amorphous phase of the fibers consist of essentially extended chain molecules with an average distance between the folds exceeding 1500Å.

The logic and reliability of this analysis has been tested by calculating the density of the strength-determining phase from the cohesive energies calculated from the experimental data of Figure 9. The results of these calculations yield for PET a value of specific cohesive energy of 1.3×10^{-13} ergs/5Å for the data obtained at 23°C and 2.0×10^{-3} ergs/5Å for the data of −100°C. The density of the strength determining phase can then be estimated using, e.g., Bunn's empirical relationship.[20]

$$(E_1 - E_2)/E_2 = 1.73\,(V_2 - V_1)/V_1$$

where E_1 and E_2 are the respective molar cohesive energies at molar volumes V_1 and V_2. The value obtained (~ 1.0) is about 30% lower than that of the amorphous PET, which represents a gratifying agreement for a study of this type.

SUMMARY AND CONCLUSIONS

A method has been developed and applied which makes possible the study of the morphology of highly-oriented polymers by analyzing the tensile response of samples having different molecular weights and similar morphological characteristics. It has been shown that the responses of highly-oriented polymers can be adequately predicted from the properties calculated for an ensemble of perfectly oriented polymer molecules.

Specifically, with regard to the morphology of highly-oriented PET and Nylon 6 fibers we have found that:

1) Highly-oriented melt spun PET and Nylon 6 fibers have a composite structure consisting of at least two distinct phases.

2) The strength of these fibers is determined primarily by the strength of the low-density phase.

3) The crystallites are embedded in the low-density matrix in a manner which results in a very inefficient reinforcement of the structure.

4) The coupling between phases approaches that of a series model.

5) The crystallites have a length to diameter ratio of less than two.

6) The strength determining low-density matrix of fully drawn fibers consists of essentially extended molecules. Estimated average distance between the random chain folds exceeds 1500Å.

References

1. R. J. E. Cumberbirch, J. Dlugosz, and F. E. Ford, *J. Textile Inst.* **52,** T513 (1961).
2. J. E. Ford, *J. Textile Inst.* **54,** T484 (1963).
3. D. C. Prevorsek, *J. Polymer Sci.* A, **1,** 993 (1963).
4. R. A. Sack, *Proc. Phys. Soc.* (London) **58,** 729 (1946).
5. D. C. Prevorsek and W. J. Lyons, *J. Appl. Phys.* **35,** 3152 (1964).
6. M. A. Miner, *J. Appl. Mech. Trans.* ASME **67,** A159 (1945).
7. D. C. Prevorsek and M. L. Brooks, *J. Appl. Polymer Sci.* **11,** 925 (1967).
8. W. J. Lyons and D. C. Prevorsek, *Textile Res. J.* **35,** 1048 (1965).
9. K. H. Meyer and W. Lotmar, *Helv. Chim. Acta.* **19,** 68 (1936).
10. W. J. Lyons, *J. Appl. Phys.* **29,** 1429 (1958).
11. L. R. G. Treloar, *Polymer* **1,** 95 (1960).
12. L. R. G. Treloar, *Polymer* **1.** 279 (1960).
13. M. A. Jaswon, P. P. Gillis and, R. E. Mark, *Proc. Roy. Soc.* **A306,** 389 (1968).
14. W. J. Dulmage and L. E. Contois, *J. Polymer Sci.* **28,** 275 (1958).
15. I. Sakurada, T. Ito and R. Nakamac, *J. Polymer Sci.* Part C **15,** 75 (1966).
16. D. C. Prevorsek and R. H. Butler, data to be published.
17. S. N. Zhurkov and E. E. Tomashevsky, *Phys. Basis of Yield and Fracture*, Ed. by A. C. Stickland, Inst. Phys. and Phys. Soc. Conference Series No. 1, London, p. 200 (1966).
18. D. C. Prevorsek and R. H. Butler, *Intern. J. Polymeric Mater.* **2,** 167 (1973).
19. P. F. Dismore and W. O. Statton, *J. Polymer Sci.* **C13,** 133 (1966).
20. C. W. Bunn, *J. Polymer Sci.* **16,** 323 (1955).
21. I. Sakurada, T. Ito, and Nacamac, *Bull. Inst. Chem. Res.* (Kyoto University) **42,** 77 (1964).